Crimson Publishers
Wings to the Research

Research Article

Titanium/Titanium Oxide Particle Dispersed W-TiC Composites for High Irradiation Applications

Eiichi Wakai[1]*, Hiroyuki Noto[2], Sho Kano[3], Shunsuke Makimura[4], Taku Ishida[4] and Tamaki Shibayama[5]

[1]J-PARC Center, Japan Atomic Energy Agency, Japan

[2]NIFS, Japan

[3]University of Tokyo, Japan

[4]J-PARC Center, KEK, Japan

[5]NIFS, Japan

ISSN: 2576-8840

***Corresponding author:** Eiichi Wakai, Division of Materials and Life Science Experimental Facility, Japan Proton Accelerator Research Complex (J-PARC) center, Japan Atomic Energy Agency (JAEA), Tokai-mura, Naka-gun, Ibaraki 319-1195, Japan

Submission: March 01, 2022

Published: March 16, 2022

Volume 16 - Issue 5

How to cite this article: Eiichi Wakai*, Hiroyuki Noto, Sho Kano, Shunsuke Makimura, Taku Ishida and Tamaki Shibayama. Toward the Creation of the Asian xEV Battery Recycling Zone. Res Dev Material Sci. 16(5). RDMS.000897. 2022. DOI: 10.31031/RDMS.2022.16.000897

Abstract

For devices and materials used in radiation environments, such as wall materials and divertors of high energy accelerator target systems under high intensity beams and fusion reactors in close proximity to high temperature plasmas, it is important to evaluate the integrity of the materials so that they can withstand large amounts of radiation and high heat loads. In this study, we investigated the irradiation resistance of a tungsten-based material, one of the candidate materials for such an environment, by mechanical alloying and high-temperature hydrostatic sintering of a high-strength W material with a grain size of 1-2μm and dispersed small titanium or titanium oxide nanoparticles. This material was irradiated up to 0.66 dpa at 500 °C. The hardness change by nanoindentation and the microstructure and atomic arrangement by scanning transmission electron microscopy were examined. Normally, this irradiation condition is known to cause significant irradiation hardening, but it was found that no irradiation hardening occurred in this material. In addition, the crystal lattice images showed lattice (atomic arrangement) distortions of less than a nanometer, but no misfit dislocations were observed. These results suggest that the formation and growth of irradiation defect clusters was suppressed by the lattice distortion formed at the nano-level or below before irradiation, and that irradiation hardening was greatly suppressed.

Keywords: Tungsten; TiC; Ti; Titanium oxide; Irradiation; Irradiation damage; Nano-indentation; STEM; Irradiation hardening; Crystal lattice distortion

Introduction

As a countermeasure against global warming and energy, research and development of innovative materials and devices are being promoted in various fields. In the fields of nuclear fusion, accelerator-targeted systems, energy, nuclear power, space environment, and radiation medicine, radiation degradation of materials and devices occurs, and thus improvements have been made from various viewpoints. For example, there are various methods such as process heat treatment, impurity addition, alloying, micro-crystallization, nanoclusters, Oxide Dispersion Strengthened (ODS) steels, composites, and nanofiber materials. These methods have improved the mechanical properties, corrosion resistance and irradiation resistance of these materials, and results have been achieved with these technologies [1-23]. In devices that receive high-density energetic particle beams, such as reactor wall materials and diver-

tors in close proximity to high-temperature plasmas and under the highest intensity beams in high-energy accelerators, it is important to evaluate the safety and lifetime of materials and devices that can withstand high thermal loads and irradiation. For materials development, a recent new research approach has been reported in development of innovative materials and measurement systems used for radiation environment [24].

Tungsten (W) has a high density (19.3g/cm^3) and extremely high melting point (3420 °C), and it has high temperature strength and the lowest coefficient of thermal expansion among metals, so it is used in fields that require heat resistance. Tungsten is one of the main materials for high temperature applications such as cathode ray tubes and rocket motor nozzles because of its high temperature strength, creep resistance, thermal conductivity, electrical resistance, vapor pressure, and thermal conductivity [25,26]. Nano and/or near-nano-sized carbide particles have been used to enhanced microstructural development and mechanical properties such as hardness and toughness [27,28]. Thus TiC has excellent properties of high hardness, good high temperature strength and good corrosion resistance. The main issues in production of Tungsten Heavy Alloys (THA) including high entropy alloying and the tungsten composites [18-20,25-33] are the high specific weight and melting point of the tungsten element, and nowadays, powder metallurgy plays one of great roles in production of these alloys and the composites.

In the field of nuclear fusion, tungsten material developments are being promoted as a part called divertor, which requires the highest heat resistance, and tungsten and the alloys and composites are also expected to be a material for the inner wall surface of the reactor wall, plasma facing materials, in contact with the plasma surface of nuclear fusion reactor [34,35], and the blistering and flaking under plasma operation will be occurred in the materials. The mechanisms are analyzed in [36-39]. In the field of high-energy accelerators that use radiation, it is used or planned as a target material for neutrons and muons, the other element particles, and research and development of materials with even higher heat resistance are underway in the world's big proton accelerator facilities such as MLF (Materials and Life Science Experimental Facility) and COMET (COherent Muon to Electron Transition) at J-PARC (Japan Proton Accelerator Research Complex) center, ESS(European Spallation Source) at Lund of Sweden, ISIS neutron and muon source at the Rutherford Appleton Laboratory of the Science and Technology Facilities Council, Mu2e (Muon-to-Electron-Conversion Experiment) at Fermilab, CSNS(China Spallation Neutron Source) at the Institute of High Energy Physics, and SNS (Spallation Neutron Source) at ORNL [6,18,40].

Tungsten is known to become brittle by recrystallization when subjected to high heat loading. In case of the fusion reactor divertor, it is expected that surface temperature would achieve as high as 1000 °C or over 1000 °C. The recrystallization embrittlement, degrading the mechanical property, is considered to be a critical issue necessary to be resolved for the divertor components development. As a solution of the problem, we have developed an oxide dispersion strengthened tungsten (ODS-W) which can avoid embrittlement even after recrystallization. It is therefore important to evaluate the integrity of the materials so that they can withstand large amounts of radiation and high heat loads. In this study, we have investigated the irradiation resistance of a tungsten-based material, one of the candidate materials for such an environment, by mechanical alloying and high-temperature hydrostatic sintering of a high-strength W material with a grain size of 1-2μm and dispersed small titanium or titanium oxide nanoparticles.

Experimental Procedure

The W-1.1wt% TiC composite was prepared using W (99.95wt% purity, particle size=1.0μm, 8100ppm oxygen (New metals and chemical co. ltd.)) and TiC (98.0wt% purity, particle size=1.8μm, <8000ppm oxygen (Japan new metals co. ltd.)). Mechanical alloying (MA) process was performed for 64hr in 360rpm using by WC ball with 3.0mm in a 250cc tungsten carbide pot with ball-powder ratio of 2:1. Since the WC pods and balls contain Co, there is a possibility that WC and Co will be mixed into the material from the wall and ball surface as the MA process progresses. After MA treatment, the specimen was formed by cold isostatic pressing and then was pre-sintered in hydrogen gas atmosphere at high temperature. The HIP treatment was carried out under the conditions of 1750 °C and 186MPa for 1.5hr. This was followed by annealing at about 1800 °C for about 1.5hrs in a vacuum (1×10^{-3}Pa). The grain size of W-1.1wt% TiC treated with 3.0mm diameter WC balls (abbreviated as W-TiC composite) was about 1-2μm, and the titanium particles of about 100nm were formed in the matrix, while titanium oxide particles were formed at the grain boundaries and ranged in size from about 100 to 500 nm. The fabrication procedure of the W-TiC composites with titanium or titanium oxide dispersed particles is shortly summarized in Figure 1.

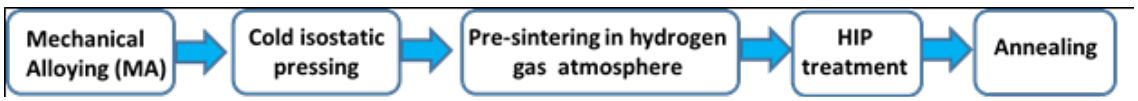

Figure 1: The fabrication procedure of the W-TiC composite with titanium or titanium oxide dispersed particles in this study.

The present W-TiC composite has dispersion-strengthened by the titanium oxide particles which are known to be stable relative to the TiC carbide particles at high temperature. The titanium oxide particles were formed because the TiC added initially reacted with impurity oxygen in tungsten matrix during the process. The hardness of W-TiC composite was 521.5±2.7 HV, respectively. The oxygen concentration in W-TiC composite was 5300ppm.

Since little work has been done on W-based titanium-based oxide dispersion strengthened (ODS), present study was performed to investigate the effect of a mechanical alloying (MA) ball diameter of 3mm on mechanical properties and microstructure after Hot Isostatic Pressing (HIP) treatment in more detail than previous studies [19,29,31]. In order to carefully investigate the effects of alloying and other elements added in the MA process, the changes in lattice parameters, matrix phase, and oxide composition and microstructure were studied in detail.

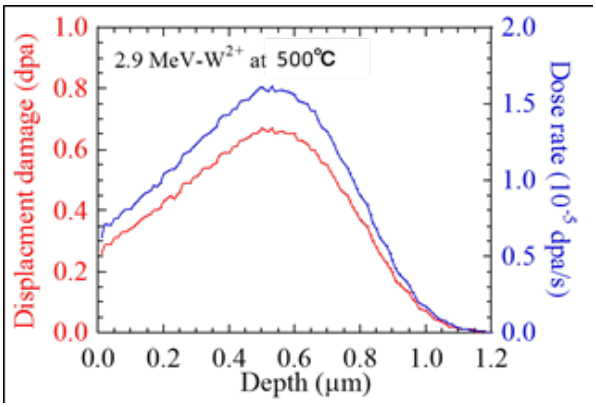

Figure 2: Displacement damage and dose rate as a function of depth in ion irradiation experiment.

For the evaluation of irradiation resistance, tungsten ion irradiation experiments were carried out at 500 °C to about 0.66dpa at the damage peak by 2.9MeV W^{2+} ions from the Tandetron accelerator at the High Fluence Irradiation Facility, the University of Tokyo (HIT). The displacement damage in W was calculated by SRIM code, the Stopping and Range of Ions in Matter [41], and the displacement damage and dose rate are shown in Figure 2. Microstructural observation and element analysis were carried out at 200kV using a Transmission Electron Microscope/Scanning Transmission Electron Microscope (TEM/STEM), the JOEL JEM-2800 with X-ray Energy Dispersive Spectroscopy (EDS), and X-ray diffraction analysis was also performed in the facility of NIFS. The nano hardness measurement was carried out using a Shimadzu nano-indenter with a Berkovich type indenter. Nano-indentation was measured at about 90 points each in the irradiated and non-irradiated mask regions of the irradiated specimen, which were valid data. In this measurement, the indentation depth was controlled, and the indentation depth was set to 0.15μm.

Results and Discussion

X-ray diffraction analysis

Figure 3 shows the X-ray diffraction spectra of W-TiC composite. In the X-ray spectrum, the main W peak, (110), was visible, but a TiO_2 (200) peak was observed overlapping to the left of it. It was found that the main peak of W-TiC composite was also generated at a slightly lower angle than usual tungsten (110). The distances of (110) plane in W-TiC composite and pure W were 0.2258nm and 0.2238nm, respectively. The lattice constant of W-TiC composite in bcc crystal structure was evaluated to be a=0.3194nm from that of W in bcc crystal structure, a=0.3165nm. Weak peaks in the (100) plane of W_2C were also observed. At the sintering temperature of 1750 °C, it seems reasonable to assume that a small amount of W_2C is formed, since W_2C is first formed in the presence of carbon. In this analysis, we referred to the results of XRD analysis of W2C by Jonda [42] for evaluation.

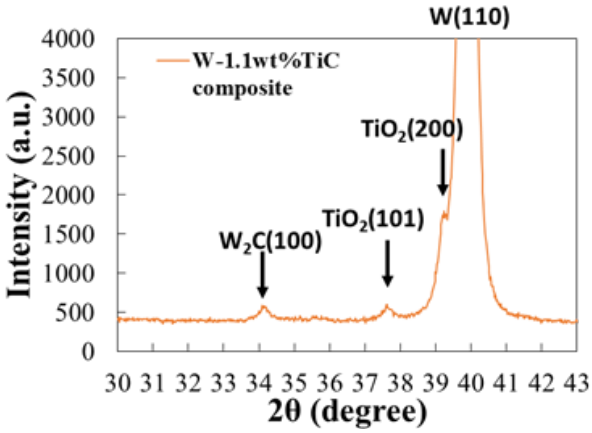

Figure 3: X-ray diffraction spectra of W-TiC composite.

Microstructures of the specimens

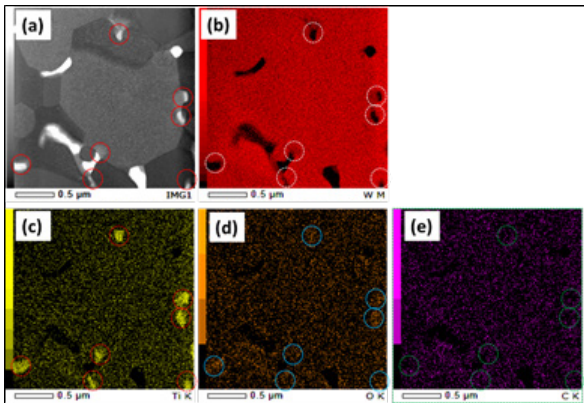

Figure 4: Image of (a) STEM and EDS mappings of (b) W, (c) Ti, (d) O, (e) C elements in W-TiC composite.

Titanium oxide was observed at grain boundaries, and titanium phases were observed within the grains, as reported in Noto's pre-

vious TEM+EDS studies. Here present study showed the mapping of the EDS images of the elemental distributions of W, Ti, O, and C in W-TiC composite as shown in Figure 4 and confirmed the correlation for each element. The areas where titanium was detected in the titanium image in Figure 4(c) are circled; similar areas are circled in the STEM images and images of other elements so that the corresponding areas can also be identified. The distribution of Ti and that of O were confirmed to be correlated to some extent, but the distribution of Ti seems to be more extensive and intense than that of O. The correlation of C and W with the other elements was not obvious. Ti particle image was also observed in the crystal grains, and in areas where precipitates were not observed, the distribution of W, Ti, C and O was almost uniformly present.

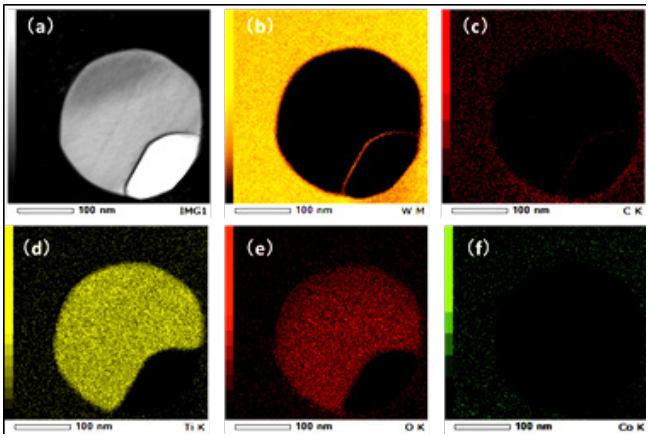

Figure 5: EDS mapping of precipitate in W-TiC composite (non-irradiated area): (a) Bright-field image, (b) W, (c) C, (d) Ti, (e) O, and (f) Co.

Magnified images of the titanium oxide formed in the crystal grains by transmission electron microscopy with EDS are shown in Figure 5. From the results of EDS analysis of the elements in the matrix and precipitates, elements such as Ti were detected in the matrix, and the precipitates mainly consisted of Ti and O at about 1:2, with about 2 at% W and a small amount of Co. In Figure 6, the other precipitate is shown, and bright-field image (a) and (c), diffraction pattern (b) and (e), and dark-filed image (d) are given. The diffraction pattern of the precipitates shows that several types of precipitates are formed. The types are classified by color with respect to the speckles of those precipitates. As seen in Figure 6(d), the detailed internal structure of the titanium oxides has microstructures with black lines, and the black area has carbon content of about 2.6 at%, but no Co was detected. In Figure 6(e), some extra spots were observed. In (d), chemical analysis in the area from 1 to 3 is given in Table 1. In this region, the Co concentration in the matrix is relatively higher than in other regions, supplementing the fact that the Co concentration in this matrix is not an average value. Since the concentrations of each element in area 1 and 3 were almost identical, it is considered that the material is TiO_2 with the same composition, although the structure may be different. All the area from 1 to 3 seem to be contaminated with tungsten. In area 2, carbon, which was not measured in area 1 and 3, was measured, suggesting that tungsten carbide or titanium carbide is mixed with titanium dioxide and is stable.

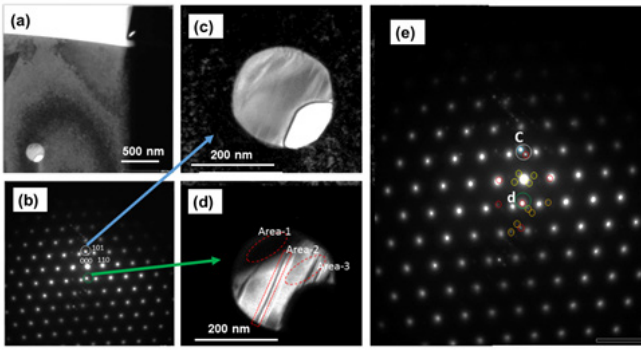

Figure 6: (a) Bright-field image, (b) diffraction pattern, (c) dark-filed image-1, (d) dark-filed image-2, (e) a magnified diffraction pattern of (c) in W-TiC composite. In the dark-field image-1, two extra spots are selected. In the dark-field image-2, one extra spot which corresponds to TiO_2 is selected.

Table 1: Chemical analysis of matrix and precipitate in W-TiC composite (non-irradiated area) measured by EDS (at%).

Position	W	Ti	O	C	Co
Matrix	91.78	1.12	2.93	0.00	4.17
Precipitate - area-1	2.22	31.73	65.60	0.00	0.44
Precipitate -area-2	2.28	30.38	64.77	2.56	0.00
Precipitate -area-3	2.12	32.42	65.04	0.00	0.41

From the results obtained data (Figures 3-5), it is thought that the increase in the lattice parameter was attributed to the incorporation of elements such as Ti into W during MA, and the alloying process was partially advanced.

Nano indentation and high resolution TEM observation for irradiated specimen

The nano hardness of W-TiC composite was 6.4±1.2GPa and 6.4±1.4GPa before and after irradiation, respectively, and no Irradiation hardening were observed.

Since it has been reported that W-based materials usually undergo irradiation hardening of about 2-3GPa even at this level of irradiation [20]. In order to investigate the cause of the irradiation hardening, the changes in the precipitation state and the disorder of the atomic arrangement in the matrix were investigated by transmission electron microscopy.

The image of the irradiation defect structure observed after ion irradiation is shown in Figure 7. No void formation could be observed. As observed by the weak-beam dark field method, interstitial dislocation loops are usually formed at this temperature, but seemed to be hardly formed in this material. Only a few black dots,

which may have been formed by irradiation, were observed as seen in Figure 7(c). Therefore, this material is considered to have a high performance against irradiation.

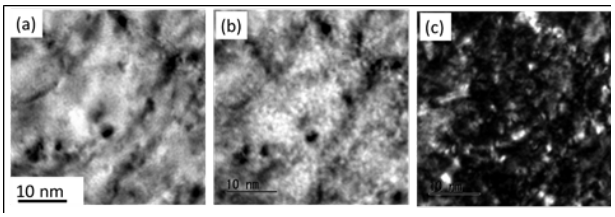

Figure 7: (a) Bright-field image (just focus), (b) bright-field image (under focus), (C) weak-beam dark field image in the irradiated W-TiC composite at 500 °C to 0.66dpa.

Figure 8 is a high-resolution lattice image of W-TiC composite. In the W-TiC composite, although the formation of irradiation-induced precipitation in the base metal was not clearly observed in the diffraction spots, local atomic arrangement distortions occurred before irradiation in many regions and remained stable after irradiation, which was presumed to be a factor for the excellent irradiation resistance, it can be seen that the atomic arrangement is disordered. However, no misfit dislocation is observed. The spacing of the (110) plane in the atomic arrangement was confirmed to be consistent with the plane crunch of the same plane measured by XRD. The region where the atomic arrangement does not appear is presumed to be the region where nano-order precipitates exist in W. These precipitates, which are thought to exist in the matrix phase in nano-order, are presumed to be the effect of W_2C, which was also observed in XRD measurements, and titanium and carbon, which were measured in EDS measurements. In addition, the diffraction spots show spots outside the matrix phase, which are thought to be due to W_2C and other elements (titanium, oxygen, carbon, and cobalt) measured by XRD and EDS.

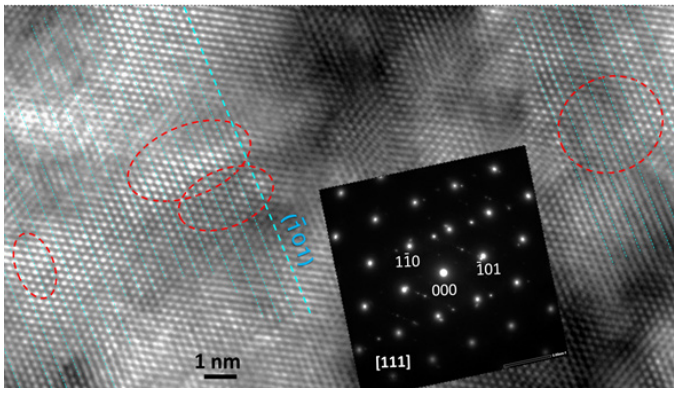

Figure 8: High resolution lattice image and the diffraction pattern of the irradiated W-TiC composite taken from [111] pole. The area circled by the red dotted line where distortions in the arrangement of atoms are visible.

Tungsten carbides (WCs) are promising candidates as nonprecious metal of hydrogen evolution reaction (HER) catalysts, owing to their stability in acidic solutions and the similarity in their electronic structures to that of Pt [43,44]. The crystalline phase of WC depends on the synthesis protocol used, and the most common phases are considered to be the most stable WC and the metastable W_2C and WC_{1-x} phases [45]. Jonda was focused on the High Velocity Oxy Fuel (HVOF) spraying with feedstock powders WC-Co-Cr, WC-Co and WC-Cr_3C_2-Ni [42]. Based on the results of the TEM analysis, the specimen coating contained an amorphous matrix and two types of precipitates: WC and W_2C. The specimen coating contained a matrix with an amorphous structure and precipitation of WC. Finally, analysis of the specimen coating showed a matrix with an amorphous structure and two types of precipitations: WC and Cr_3C_2. The XRD studies showed that phase composition of cermet coatings consisted of hexagonal WC, hexagonal W_2C carbide, hexagonal cobalt and a cubic solid solution of tungsten in cobalt with composition $Co_{0.9}W_{0.1}$. Additionally, in the WC-Cr_3C_2-Ni coating, Cr_3C_2 and Cr_7C_3 carbides were identified. In present study system of W, C and Ti with the influence of high oxygen concentration, it will be important in the future to further control the microstructure, referring to the study and analysis of the control of powder in W-based alloys by Jonda et al. [42].

In any case, the new W-TiC composites fabricated in this study were found to have very high resistance to irradiation and are expected to be used in various devices used in severe radiation environments. It is important to proceed with further development, including further improvement and increase in production volume.

Conclusion

In this study, the irradiation resistance of tungsten-based materials was evaluated by mechanical alloying and high-temperature hydrostatic sintering of small titanium or titanium oxide nanoparticles dispersed in high-strength W material (W-TiC composite with small titanium or titanium oxide nanoparticles) with a grain size of 1-2μm. The material was irradiated at 500 °C up to 0.66dpa. Hardness changes by nanoindentation and microstructure and atomic arrangement observations by scanning transmission electron microscopy showed that no irradiation hardening occurred in this material, although it is known that significant irradiation hardening usually occurs under these irradiation conditions. In the crystal lattice images, lattice (atomic arrangement) distortions of less than one nanometer were observed, but no misfit dislocations were observed. Present result suggests that the formation of lattice distortions below the nanometer level prior to irradiation suppressed the formation and growth of irradiation defect clusters and significantly reduced irradiation hardening. Since this type of material was found to have attractive properties, we plan to further improve the material by conducting further irradiation resistance tests, thermal load tests, various strength tests, and microstructure observations.

Acknowledgement

This study was supported by Kakenhi (21H04480 and 21H04668), collaborative research program of National Institute for Fusion Science, and the Japan-U.S. Science and Technology Cooperation Program (High Energy Physics).

Conflict of Interest

The authors declare no conflict of interest.

References

1. Ozturk F, Bas O, Ates E (2021) Thermoplastic composite materials for the aerospace industry. Research & Development in Material Science 15: 1745-1748.
2. Silva PM, Serna MM, Galego E and Faria Jr RN(2021) The influence of the nanostructures on the dye adsorption in dye sensitized solar cell. Research & Development in Material science 15(2): 000859.
3. Wakai E, Taguchi T, Yamamoto T, Tomita H, Takada F, et al. (2005) Effects of helium production and heat treatment on neutron irradiation hardening of F82H steels irradiated with neutrons. Materials Transactions JIM 46(3): 481-486.
4. Ishida T, Wakai E, Makimura S, Hurh PG, Ammigan K, et al. (2020) Radiation damage studies on titanium alloys as high intensity proton accelerator beam window materials. JPS Conference Proceedings 28: 041001.
5. Ishida T, Wakai E, Hagiwara M, Makimura S, Tada M, et al. (2018) Study of the radiation damage effect on Titanium metastable beta alloy by high intensity proton beam. Nuclear Materials and Energy 15: 169-174.
6. Sato K, Wakai E, Makimura S, Saito S, Ishida T, et al. (2020) Introduction of this conference. Proceedings of 14th International Workshop Spallation Materials Technology. JPS conference proceedings 28: 021001.
7. Wakai E, Hishinuma A, Usami K, Kato Y, Takaki S, et al. (2000) Damage structures and mechanical properties of high-purity Fe-9Cr alloys irradiated by neutrons. Materials Transactions JIM 41 (9): 1180-1183.
8. Wakai E, Ando M, Okubo N, (2015) Effects of heat treatments and addition of minor elements of boron and nitrogen on mechanical properties and microstructures of reduced-activation ferritic/martensitic steel. Journal of Plasma and Fusion Research Series 11: 104-112.
9. Okubo N, Wakai E, Matsukawa S, Sawai T, Kitazawa S, et al. (2007) Effects of heat treatment and irradiation on mechanical properties in F82H steel doped with boron and nitrogen. Journal of Nuclear Materials 367-370: 107-111.
10. Chauhan A, Litvinov D, Carlan, Y, Aktaa J (2016) Study of the deformation and damage mechanisms of a 9Cr-ODS steel: Microstructure evolution and fracture characteristics. Materials Science and Engineering: A 658: 123-134.
11. Laurent-Brocq M, Legendre FL, Mathon MH, Mascaro A, Poissonnet S, et al. (2012) Influence of ball-milling and annealing conditions on nanocluster characteristics in oxide dispersion strengthened steels. Acta Materialia 60(20): 7150-7159.
12. Klueh RL, Shingledecker JP, Swindeman RW, Hoelzer, DT (2005) Oxide dispersion-strengthened steels: A comparison of some commercial and experimental alloys. Journal of Nuclear Materials 341(2-3): 103-114.
13. Zinkle SJ, Busby JT (2009) Structural materials for fission & fusion energy. Materials today 12(11): 12-19.
14. Moriyama T, Yoshimi K, Zhao M, Masnou T, Yokoyama T, et al. (2017) Room-temperature fracture toughness of MoSiBTiC alloys. Intermetallics 84: 92-102.
15. Taguchi T, Igawa N, Miwa S, Wakai E, Jitsukawa S, et al. (2004) Synergistic effects of implanted helium and hydrogen and the effect of irradiation temperature on the microstructure of SiC/SiC composites. Journal of Nuclear Materials 335(3): 508-514.
16. Snead LL, Nozawa T, Katoh Y, Byun TS, Kondo S, et al. (2007) Handbook of SiC properties for fuel performance modeling. Journal of Nuclear Materials 371 (1-3): 329-377.
17. El-Atwani O, Nathaniel JE, Leff AC, Hattar K, Taheri ML (2017) Direct observation of sink-dependent defect evolution in nanocrystalline ion under irradiation. Scientific Reports 7: 1836.
18. Makimura S, Kurishita H, Niikura K, Jung H, Onoi M, et al. (2020) Tungsten alloy development as advanced target material for high-power proton accelerator. JPS Conference Proceedings 28: 031002.
19. Noto H, Hishinuma Y, Muroga T, Benoki H (2020) Microstructure and mechanical properties of dispersion strengthened tungsten by HIP treatment followed by thermal annealing. Results in Materials 7: 100116.
20. Nogami S, Hasegawa A, Fukada M, Rieth M, Reiser J, et al. (2021) Mechnical properties of tungsten: Recent research on modified tungsten materials in Japan. Journal of Nuclear Materials 543: 152506.
21. Teru T, Wakeda M, Suzudo T, Itakura M, Ogata S (2020) Anomalous solution softening by unique energy balance mediated by kink mechanism in tungsten-rhenium alloys. Journal of Applied Physics 127: 025101.
22. Cui S, Cui C, Xie J, Liu S, Shi J (2018) Carbon fibers coated with graphene reinforced TiAl alloy composite with high strength and toughness. Scientific Reports 8: 2364.
23. Viswanathan R (2004) Materials technology for coal fired power plants. Advanced Materials and Processes 162(8): 73-76.
24. Wakai E, Iwamoto Y, Shibayama T, Sato K, Toyota, et al. (2022) Development of innovative materials and measurement systems used for radiation environment. Research & Development in Material Science 16(4): 1859-1867.
25. Reiser J, Rieth M, Dafferner B, Hoffmann A (2012) Tungsten foil laminate for structural divertor applications-basics and outlook. Journal of Nuclear Materials 423(1-3): 1-8.
26. Greger M, Čížek L, Widomská M (2004) Structure and mechanical properties of formed tungsten based materials. Journal of Materials Processing Technology 157: 683-687.
27. Myalska H, Dybowski B, Moskal G (2017) W-Co coatings and sinters modified with nano-sized tic microstructure - quantitative evaluation. Advances in Science and Technology Research Journal 11(1): 220-231.
28. Kacmaz D, Kalkavan F, Yazaici S, Demirural A, Baykara T (2019) Processing, sintering and performance of WC-Co-Near-Nano TiC metal matrix composites. Research & Development in Material Science 9: 1012-1018.
29. Noto H, Hishinuma Y, Muroga T, Tanaka T (2021) Thermal change of microstructure and mechanical properties of dispersion strengthened tungsten. Nuclear Fusion 61: 116001.
30. Kurishita H, Arakawa H, Matsuo S, Sakamoto T, Kobayashi S, et al. (2013) Development of nanostructured tungsten-based materials resistant to recrystallization and/or radiation induced embrittlement mater. Trans 54: 456-465.
31. Noto H, Hishinuma Y, Muroga T, Benoni H (2020) Formation mechanism of nano-strengthening particles in dispersion strengthened W-Ti alloys. Plasma and Fusion Research 15: 1205021.
32. El-Atwani O, Li N, Li M, Devaraj A, Baldwin JKS, et al. (2019) Outstanding radiation resistance of tungsten-based high-entropy alloys. Science Advances 5: eaav2002.
33. Lu ZP, Wang H, Chen MW, Baker I, Yeh JW, et al. (2015) An assessment on the future development of high-entropy alloys: Summary from a

recent workshop. Intermetallics 66: 67-76.

34. Sagara A. Tamura H, Tanaka T, Yanagi N, Miyazawa J, et al. (2014) Helical reactor design FFHR-d1 and c1 for steady-state DEMO. Fusion Engineering and Design 89: 2114-2120.

35. Tokitani M, Hamaji Y, Hiraoka Y, Masuzaki S , Tamura H, et al. (2021) Advanced multi-step brazing for fabrication of a divertor heat removal component. Nuclear Fusion 61: 046016.

36. Shu WM, Wakai E, Yamanishi T (2007) Blister bursting and deuterium bursting release from tungsten exposed to high fluences of high flux and low energy deuterium plasma. Nuclear Fusion 47 (3): 201-209.

37. Shu WM, Kawasuso A, Miwa Y, Wakai E, Luo GN, et al. (2007) Microstructure dependence of deuterium retention and blistering in the near-surface region of tungsten exposed to high flux deuterium plasmas of 38eV at 315K. Physica Scripta 2007 (T128): 96-99.

38. Wakai E, Ezawa T, Takenaka T, Imamura J, Tanabe T, et al. (2007) Effect of solute elements in Ni alloys on blistering under He+ and D+ ion irradiation. Journal of Nuclear Materials 367: 478-482.

39. Wakai E, Ezawa T, Imamura J, Takenaka T, Tanabe T, et al. (2002) Effect of solute atoms on swelling in Ni alloys and pure Ni under He+ ion irradiation. Journal of Nuclear Materials 307-311: 367-373.

40. Wakai E, Takaya S, Matsui Y, Nagae Y, Kato S, et al. (2021) Irradiation damages of structural materials under different irradiation environments. Journal of Nuclear Materials 543: 152503.

41. Ziegler JF, Ziegler MD, Biersack JP (2010) SRIM - The stopping and range of ions in matter. Nuclear Instruments and Methods in Physics Research Section B: Beam Interactions with Materials and Atoms 268: 1818-1823.

42. Jonda E, Latka L, Tomiczek A, Godzierz M, Pakieta W, et al. (2022) Microstucture investigation of WC-based coatings prepared by HVOF onto AZ31 substrate. Materials 15: 40.

43. Bennett LH, Cuthil JR, McAlister AJ, EricksonNE, Watson RE (1974) Electronic structure and catalytic behavior of tungsten carbide. Science 184: 563-565.

44. Weidman MC, Esposito DV, Hsu YC, Chen JG (2012) Comparison of electrochemical stability of transition metal carbides (WC, W2C, MosC) over a wide pH range. Journal of Power Sources 202: 11-17.

45. Neylon MK, Choi S, Kwon H, Curry KE, Thomson LT (1999) Catalytic properties of eary transition metal nitrides and carbides: n-Butane hydrogenolysis, dehydrogenation and isomerization. Applied Catalysis A 183: 253-263.